Bond Graph Modeling and Simulation of a Dual-Arm Mobile Manipulator

Yang Qian, Ahmed Rahmani

LAGIS UMR 8219 CNRS,
Ecole Centrale de Lille
59650 Villeneuve d'Ascq, France
yang.qian@ec-lille.fr, ahmed.rahmani@ec-lille.fr

Abstract—**This paper presents a methodology for dynamic modeling and trajectory tracking of a nonholonomic wheeled mobile manipulator with dual arms. First, the kinematic model is set up based on modified D-H principle. Then we employ an energy-based approach for modeling and its bond graph notation ensures encapsulation of functionality, extendibility and reusability of each element of the model. A toolbox BG V.2.1 in Matlab/Simulink is used for simulation and validation. Simulation results are performed to illustrate the efficacy of the proposed dynamic model.**

Keywords—Bond graph modeling, mobile manipulator, dual-arm, trajectory tracking

I. INTRODUCTION

In recent years, the study of personal assistant robot with dexterous arms is a very active area in robotics. The project underway pursues the prototype development of a personal assistant robot for assistance tasks in household environments. It is a complex machine that consists of a mobile platform, two robotic arms and two dexterous hands. This type of robot is called a mobile manipulator [1-6]. Due to the mobility of the platform and the manipulability of the arms, the robot is capable of performing dexterous manipulation tasks. However, this kind of mobile manipulator needs to deal with more complicated control problems, such as trajectory tracking, trajectory planning, cooperation, compliance, motion constraints called nonholonomic, and manipulability, etc. Modeling is usually treated as a preprocessing stage for the application of a control strategy. As a part of the project, this paper presents a methodology for dynamic modeling and trajectory tracking of the nonholonomic wheeled mobile manipulator with dual arms (without hands).

There are several fundamental methods applied to complex robots to formulate the equations of motion, such as Newton-Euler formulation [7], Euler-Lagrange principle [8], Kane's method [9], and Screw theory [10]. Usually mathematical models have thousands of equations so that these models are difficult to create and even more difficult to maintain. Bond graph represents a graphical modeling language to model physical systems of arbitrary types such as electrical, mechanical, magnetic, fluid, chemical, and thermodynamic systems. This means that systems from different domains can be described in the same way. Many researchers have worked on bond graph and its notation can be found in [11-13].

Bond graph notation ensures encapsulation of functionality, extendibility and reusability of each element of the model. As a result this method is generally more suitable for the modeling of complex robotic systems like mobile manipulators than equation-based modeling. Similar work has been done. In [14] bond graph method has been applied to model the mechanical dynamics of an excavating manipulator which is modeled as a 3 DOFs planar manipulator. This is done by applying forward recursive equations similar to those applied in Newton-Euler method only to determine the centroid velocities of the links. In [15] the dynamic behavior of the youBot (mobile manipulator robot) is decomposed into three types of components: Mecanum wheels, joints of the manipulator and links of the manipulator. The kinematic representation of mechanical elements is captured using screw theory. Although significant research has been done on modeling of different robots by bond graph, no one has established a complete bond graph model for the personal assistant robot.

In this paper, the bond graph model is build step by step following the Newton-Euler formalism for the dual-arm mobile manipulator system. Bond graphs are used to represent the dynamics of each part including the mobile platform, the arms and the electromechanical system. The paper is organized as follows. In Section II we introduce the mechanical structure of a dual-arm mobile manipulator. In Section III we derive the constraint equations and set up the kinematic model. Section IV provides the modeling process for the whole robot. A simulation case is analyzed in Section V. Finally, Section VI concludes with the main points made in this paper.

II. MOBILE MANIPULATOR: MECHANICAL STRUCTURE DESIGN AND MODEL DRAWING

We target our robot consisting of a mobile platform equipped with dual-arm/hand system with adequate payload and dexterity characteristics. For example, the mobile base should be able to transit doors and navigate in human-sized environments. The fingertips of the dexterous hands should reach a reasonable fraction of the workspace reachable by a standing person and possibly be able to pick up objects on the ground. For realizing the capabilities

mentioned above, our human-like mobile manipulator prototype roughly stands 140 cm tall and weighs 80 kg. Fig. 1 shows its dimensions. The high number of DOFs provides the robot with the ability of realizing complex motions. Fig. 2 and Fig. 3 describe the structures of the mobile platform and the robotic hand.
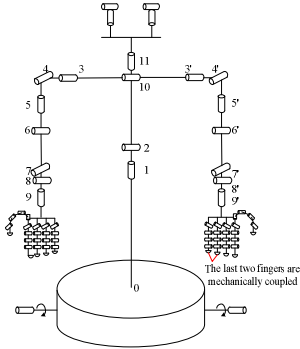
Fig. 1. Dimensions of robot model

TABLE I. DOFs CONFIGURATION

Part	DOF
Eyes	2 (pan-tilt) ×2
Neck	2
Waist	2
Arms	7×2
Hands	16×2
Mobile base	2

The model drawn in Solidworks is shown in Fig. 4. Each part's size and shape of this robot are created as those of the actual component. Only the mechanical parts are included in the Solidworks drawing. This structure is sufficient to reflect the physical properties of the mobile manipulator, which will be examined later.
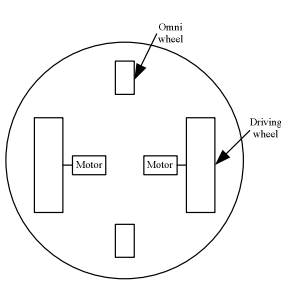
Fig. 2. Structure of mobile platform
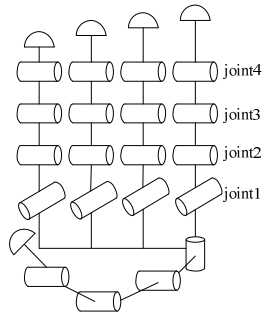
Fig. 3. Structure of dexterous robotic hand
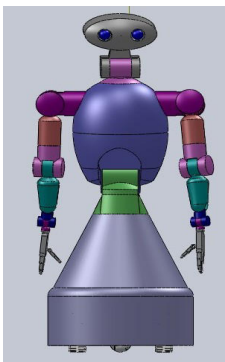
Fig. 4. Solidworks drawing of mobile manipulator
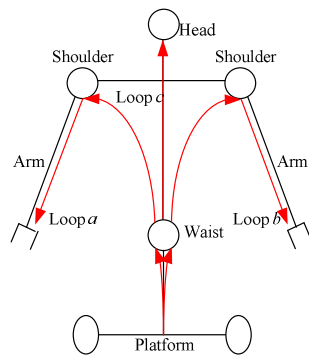
Fig. 5. Kinematic loops without fingers

III. KINEMATICS ANALYSIS

Before bond graph modeling, the kinematic equations are discussed briefly. The mobile part and the manipulator part are discussed separately. In this paper, we neglect the effect of the dexterous hands. For the extendibility of bond graph, the models of the hands are easily added to the entire bond graph model.

Neglecting the dexterous hands, the robot's links and joints can be divided into five main parts: mobile platform, waist, left arm, right arm and head. As shown in Fig. 5, three kinematic loops are formulated:

Loop a: it contains platform, waist, right shoulder and right arm.

Loop b: it contains platform, waist, left shoulder and left arm.

Loop c: it contains platform, waist, neck and head.

Note that, in the following section, Loop c will be neglected and not be simulated because it just supports the vision system. In this paper, q denotes the vector of generalized coordinates of Loop a and Loop b and may be separated into four sets $q = \begin{bmatrix} q_v^T & q_w^T & q_r^T & q_l^T \end{bmatrix}^T \in \Re^p$. The subscripts v, w, r and l represent the mobile platform, waist, right arm and left arm respectively. $q_v \in \Re^m$ describes the vector of generalized coordinates of mobile platform, $q_w \in \Re^n$ is the vector of generalized coordinates of the waist, and $q_r, q_l \in \Re^a$ are the vectors of generalized coordinates of the right and left arms respectively.

A. Mathematical model of differential wheeled platform

As described in the mechanical design process, the platform has two driving wheels (conventional wheels) and two passive supporting wheels (omni wheels) (Fig. 6). $\begin{bmatrix} x_c & y_c \end{bmatrix}^T$ are the coordinates of the center of mass in the world coordinate system, ϕ is the heading angle of the platform measured from the x-axis of the world coordinate system, ω_c is the angular velocity of the mobile platform, b is the distance between the driving wheels and r is the radius of each driving wheel.
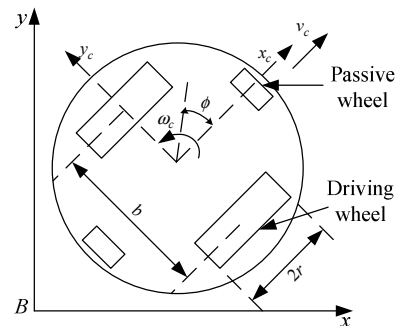
Fig. 6. Schematic of differential wheeled robot

The nonholonomic constraint states that the robot can only move in the direction normal to the axis of the driving

wheels, i.e., the mobile base satisfies the conditions of pure rolling and non slipping [16]:

$$\dot{y}_c \cos\phi - \dot{x}_c \sin\phi = 0 \quad (1)$$

Let the Lagrange coordinates of the mobile platform be $q_v = \begin{bmatrix} x_c & y_c & \phi \end{bmatrix}^T$ which represent the position of the robot in the world coordinate system, the constraint can be written in the form:

$$A_v(q_v)\dot{q}_v = 0 \quad (2)$$

which is according to (1), where $A_v(q_v) = \begin{bmatrix} -\sin\phi & \cos\phi & 0 \end{bmatrix}$.

B. Forward kinematics of a manipulator

As mentioned above, without the dexterous hands, the robot can be divided into three independent loops. For the body (excluding mobile platform), each loop is considered as a linkage, which is defined to be a set of attached rigid bodies. Let us take Loop a as an example. Each rigid body is referred to as a link, denoted by W. Let W_1, W_2, . . ., W_{n+a} denote a set of $n+a$ links. Let $Q = \begin{bmatrix} q_w^T & q_r^T \end{bmatrix}^T = \begin{bmatrix} q_1 & q_2 & ... & q_{n+a} \end{bmatrix}^T$ denote the set of angles of rotational joints, then Q yields an acceptable position and orientation of the links in the chain by using the homogeneous transformation matrix. Given the matrix $^{i-1}T_i$ expressing the difference between the coordinate frame of W_{i-1} and the coordinate frame of W_i, the application of $^{i-1}T_i$ transforms any point in W_{i-1} to the body frame of W_i. Repeating the above procedure, the end-effector location $\begin{bmatrix} x' & y' & z' \end{bmatrix}^T$ in the frame Σ_0 attached to the mobile base is determined by multiplying the transformation matrices and the end-effector location $\begin{bmatrix} x & y & z \end{bmatrix}^T \in W_{n+a}$:

$$\begin{bmatrix} x' & y' & z' & 1 \end{bmatrix}^T = {}^0T_1\,{}^1T_2...{}^{n+a-1}T_{n+a} \begin{bmatrix} x & y & z & 1 \end{bmatrix}^T \quad (3)$$
$$= T \begin{bmatrix} x & y & z & 1 \end{bmatrix}^T$$

where $T = \begin{bmatrix} {}^0R_{n+a} & {}^0P_{n+a} \\ 0...0 & 1 \end{bmatrix} = \begin{bmatrix} n_x & o_x & a_x & p_x \\ n_y & o_y & a_y & p_y \\ n_z & o_z & a_z & p_z \\ 0 & 0 & 0 & 1 \end{bmatrix} \in \Re^{4\times4}$,

$^0R_{n+a} = \begin{bmatrix} n_x & o_x & a_x \\ n_y & o_y & a_y \\ n_z & o_z & a_z \end{bmatrix} \in \Re^{3\times3}$ and

$^0P_{n+a} = \begin{bmatrix} p_x & p_y & p_z \end{bmatrix}^T \in \Re^3$ give the rotation axis and the position in the frame Σ_0, respectively.

The above formula represents the forward kinematics for positioning a linkage by a specific joint configuration.

The Modified Denavit-Hartenberg method (MDH) [17] is used to analyze the kinematics. This method is commonly used in literature dealing with manipulator kinematics. Fig. 7 illustrates the idea of attaching frames of the mobile manipulator according to MDH. The frame $x_0 y_0 z_0$ is attached to the mobile base. The other frames are attached to each link.
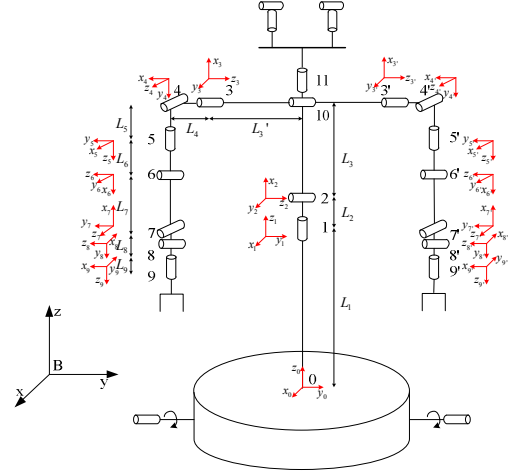
Fig. 7. Coordinate frames attached to mobile manipulator

IV. BOND GRAPH MODELING

This section presents the activities related to bond graph modeling of the whole mobile manipulator. For the sake of clarity, first, the concept of bond graph is discussed. Associated with each bond are power conjugates, effort and flow, the product of which is the instantaneous power flowing to or from physical elements. Efforts and flows in mechanical systems are forces and velocities. Energy dissipation is modeled by resistive element **R**, energy storage devices such as springs and inertia are modeled by elements **C** and **I**, sources of efforts and flows are represented by **Se** and **Sf**, and power transformations are modeled by transformers **TF** or gyrators **GY**. Power bonds join at **0** junctions summing flows to zero with equal efforts or at **1** junctions summing efforts to zero with equal flows, which implements Newton's 2nd law. Bond graphs have many advantages. Multiphysic dynamic systems such as electrical, mechanical, magnetic, fluid, chemical, and thermodynamic systems can be modeled and linked together. Bond graph is an energy-based modeling technique with modularity that permits system growth. Note that the dual-arm mobile manipulator is a very complex electromechanical system. This method is suitable for its modeling.

The modeling process contains four steps: modeling an electromechanical system, modeling joints, modeling links and modeling Eulerian Junction Structure (EJS).

A. Modeling of Electromechanical System

An electromechanical system can be considered as a concatenation of four parts: electrical part of DC motor, mechanical part of DC motor, gear set and load part. The word bond graph model is given by Fig. 8. Fig. 9 describes the bond graph model of the electromechanical part. The electrical part consists of three components resistance R_a,

inductance L_a and an input effort source U which represents the voltage source of the motor. The gyrator GY describes the electromechanical conversion in the motor. The mechanical part is characterized by its inertia I_a and viscous friction coefficient B_m. The transmission elasticity of the shaft is represented by the element $C = 1/K$. TF with a reducer constant k_r models the gearbox. The load part (joint) is characterized by its inertia J and viscous friction coefficient B.
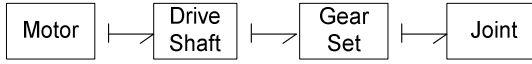
Fig. 8. Word bond graph of electromechanical system
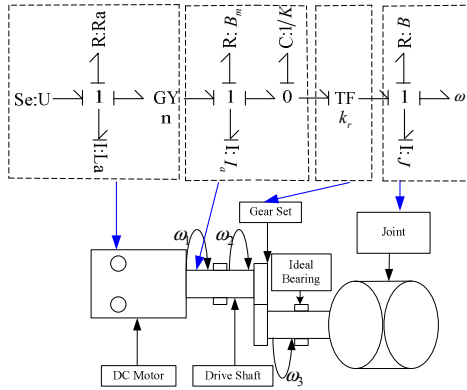
Fig. 9. Schematic of electromechanical system

B. Modeling of Mobile Platform

A mobile platform consists of left and right wheel drive subsystems and a rigid chassis. The bond graph for a differential wheeled robot is shown in Fig. 10. The 1-junctions represent the common velocity points, e.g., the rotational velocity of the left wheel $\dot{\theta}_l$, the rotational velocity of the right wheel $\dot{\theta}_r$, the forward velocity of the robot v_c, and the rotational velocity of the rigid chassis ω_c. The 0-junctions represent the common force points, e.g., the forces on the left and right sides of the robot, F_l and F_r. The wheel subsystems include the flow sources (Sf_l and Sf_r), and the inertial elements (I) that model the wheel mass m_w and the inertia I_{wl}, I_{wr}. The resistive elements (R) (with parameters R_l and R_r) model the energy dissipation (i.e., friction) in the wheels. The transformers (TF) model the transformations between the linear and rotational velocities. The chassis subsystem includes the inertia components that model its mass m_c and rotational inertia I_c.
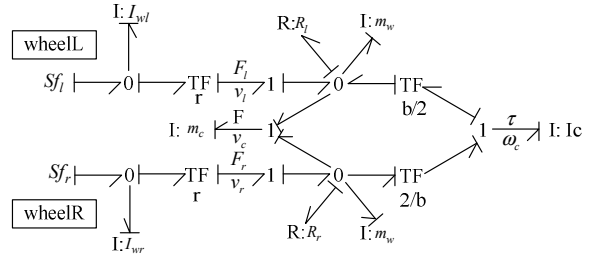
Fig. 10. Bond graph model of differential wheeled mobile robot

C. Modeling of a Manipulator

Manipulator is a chain of rigid bodies (links) connected by revolute joints.

1) Modeling of Joint

For modeling a joint, it is decided only to model the transfer of energy in a joint. Therefore, the following behavior has explicitly been neglected: (1) friction in the joint, and (2) energy storage in the joint.

Since a joint establishes a connection between two links, it imposes a relation between the angular velocities and the moments of the two bodies. A torque applied in a joint is applied between the two connected links and, in fact, applies the same torque to both links. This specifies the relation between the torque applied by the actuator ($^i\tau_{acti}$) and the torques applied to the connected links ($^i\tau_{joint\,i,i-1}$ and $^i\tau_{joint\,i,i}$):

$$^i\tau_{acti} = {}^i\tau_{joint\,i,i-1} = {}^i\tau_{joint\,i,i} \tag{4}$$

On the other hand, there is a relation between the angular velocities of $^i\omega_{i-1}$ and $^i\omega_i$. Just as with other flow type variables the following relation holds:

$$^i\omega_i = {}^i\omega_{i-1} + {}^i\omega_{acti} \tag{5}$$

In this paper $^i a_j$ denotes the value a of link j expressed in frame i. Thus $^i\omega_i$ and $^i\omega_{i-1}$ are respectively the angular velocity of link i expressed in frame i and the angular velocity of link $i-1$ expressed in frame i. $^i\omega_{acti}$ denotes the angular velocity generated by the motor. The above two relations are represented by 0-junction in the bond graph language described in Fig. 11 (a) and (b).
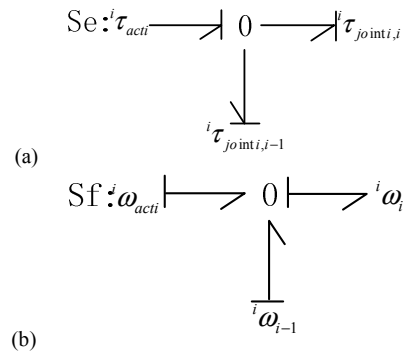
Fig. 11. Bond graph of a joint (a) effort source (b) flow source

2) Modeling of Link
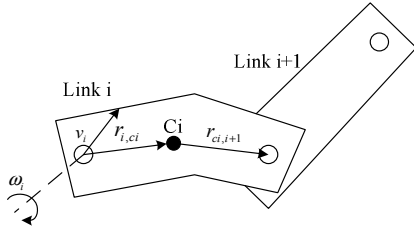
Fig. 12. Velocity relation between links
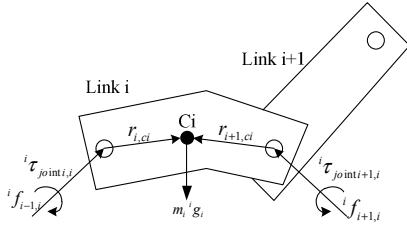
Fig. 13. Force relation between links

The velocities of link i are completely determined by the velocities of link i-1 and the motion of joint i. Fig. 12 describes the velocity relation between links.

Angular velocity of link i

$$^i\omega_i = {}^iR_{i-1}({}^{i-1}\omega_{i-1} + {}^{i-1}\omega_{acti}) \tag{6}$$

Translational velocity of link i:

$$^iv_{ci} = {}^iR_{i-1}{}^{i-1}v_i + \tilde{r}_{i,ci}{}^i\omega_i \tag{7}$$

$$^iv_{i+1} = {}^iv_{ci} + \tilde{r}_{ci,i+1}{}^i\omega_i \tag{8}$$

where c_i denotes the center of mass of link i; point i and i+1 denote the i_{th} and $(i+1)_{th}$ connection points between links; $^{i-1}\omega_{i-1}$ is the angular velocity of link $i-1$ expressed in frame $i-1$; $^iv_{ci}$, $^{i-1}v_i$ and $^iv_{i+1}$ are the linear velocities of the centre of mass of link i expressed in frame i, frame origin of link i expressed in frame $i-1$ and frame origin of link $i+1$ relative to frame i respectively; $^iR_{i-1}$ is the rotation matrix between frames i and $i-1$; $r_{i,ci}$ is a vector from point i to point ci; similarly, $r_{ci,i+1}$ is a vector from point ci to point $i+1$.

The skew-symmetric matrices $\tilde{r}$ is built from r such that

$$r = \begin{bmatrix} r_1 \\ r_2 \\ r_3 \end{bmatrix}, \tilde{r} = \begin{bmatrix} 0 & r_3 & -r_2 \\ -r_3 & 0 & r_1 \\ r_2 & -r_1 & 0 \end{bmatrix}$$

3) Newton-Euler Equations

Fig. 13 shows link i together with all forces and torques acting on it. In this figure, m_i is the mass of link i and ^ig_i is the gravitational acceleration expressed in frame i. By

the law of action and reaction $^if_{i-1,i}$ and $^if_{i+1,i}$ are respectively the force acting from link (i-1) on link i and the force acting from link (i+1) on link i expressed in frame i. As shown in (4), $^i\tau_{joint\,i,i}$ and $^i\tau_{joint\,i+1,i}$ are the torques applied by the actuator relative to frame i. When all vectors in Fig. 13 are expressed in frame i, the total force and torque applied to a link can be stated as

Total force applied to a link:

$$^iF_i = {}^if_{i-1,i} + {}^if_{i+1,i} + m_i{}^ig_i \tag{9}$$

Total torque applied to a link:

$$^i\tau_i = {}^i\tau_{joint\,i,i} + {}^i\tau_{joint\,i+1,i} + \tilde{r}_{i,ci}{}^if_{i-1,i} + \tilde{r}_{i+1,ci}{}^if_{i+1,i} \tag{10}$$

4) Eulerian Junction Structure in 3D Mechanical Systems

From (9) and (10), the coordinates of the forces and the torques are all written relative to a body-fixed frame attached at the center of mass instead of with respect to an inertial frame. In this way, the inertial tensor remains constant. Hence, we can formulate the d'Alembert principle in a body-fixed coordinate system without updating the inertial tensor. However, we now must calculate the relative coordinate transformations across joints. We must also take into account the gyroscopic torques and forces that result from formulating the d'Alembert principle in an accelerated frame. The nonlinear differential equation (11) known as Newton-Euler's equations derived by applying D'Alembert principle represent the body motion in the 3D local frame.

$$
\begin{aligned}
^i\tau_{ix} &= {}^iJ_{ixx}{}^i\dot{\omega}_{ix} + {}^i\omega_{iy}{}^iJ_{izz}{}^i\omega_{iz} - {}^i\omega_{iz}{}^iJ_{iyy}{}^i\omega_{iy} \\
^i\tau_{iy} &= {}^iJ_{iyy}{}^i\dot{\omega}_{iy} + {}^i\omega_{iz}{}^iJ_{ixx}{}^i\omega_{ix} - {}^i\omega_{ix}{}^iJ_{izz}{}^i\omega_{iz} \\
^i\tau_{iz} &= {}^iJ_{izz}{}^i\dot{\omega}_{iz} + {}^i\omega_{ix}{}^iJ_{iyy}{}^i\omega_{iy} - {}^i\omega_{iy}{}^iJ_{ixx}{}^i\omega_{ix} \\
^iF_{ix} &= m_i{}^i\dot{v}_{cix} + m_i{}^i\omega_{iy}{}^iv_{ciz} - m_i{}^i\omega_{iz}{}^iv_{ciy} \\
^iF_{iy} &= m_i{}^i\dot{v}_{ciy} + m_i{}^i\omega_{iz}{}^iv_{cix} - m_i{}^i\omega_{ix}{}^iv_{ciz} \\
^iF_{iz} &= m_i{}^i\dot{v}_{ciz} + m_i{}^i\omega_{ix}{}^iv_{ciy} - m_i{}^i\omega_{iy}{}^iv_{cix}
\end{aligned}
\tag{11}
$$

where $^iF_{ix,iy,iz}$ are the components of ^iF_i, $^i\tau_{ix,iy,iz}$ are the components of $^i\tau_i$ and $^iJ_{ixx,iyy,izz}$ are the components of ^iJ_i which is the moment of inertia of link i about its center of mass. All the forces $^iF_{ix,iy,iz}$, the torques $^i\tau_{ix,iy,iz}$ and the inertial tensor $^iJ_{ixx,iyy,izz}$ are written relative to the body-fixed frame. ^iF_i and $^i\tau_i$ have been derived in (9) and (10).

Euler's equations for the rotation of a rigid body contain a term with an exterior product between the momentum and the angular velocity. This term is associated with the gyroscopic moments M_{gyro}. The common bond graph representation of this exterior product in Euler's equations is the EJS. For the torques it is denoted by EJS-T:

Proceedings of the 1st International and 16th National Conference on Machines and Mechanisms (iNaCoMM2013), IIT Roorkee, India, Dec 18-20 2013

66

$$M_{gyro-T} = {}^i\omega_i \times {}^iJ_i\,{}^i\omega_i \qquad (12)$$

where

$${}^iJ_i = \begin{bmatrix} {}^iJ_{ixx} & 0 & 0 \\ 0 & {}^iJ_{iyy} & 0 \\ 0 & 0 & {}^iJ_{izz} \end{bmatrix} \text{ and } {}^i\omega_i = \begin{bmatrix} {}^i\omega_{ix} & {}^i\omega_{iy} & {}^i\omega_{iz} \end{bmatrix}^T.$$

From (12), the following expression can be derived:

$$M_{gyro-T} = \begin{bmatrix} M_1 \\ M_2 \\ M_3 \end{bmatrix} = \begin{bmatrix} 0 & {}^iJ_{izz}\,{}^i\omega_{iz} & -{}^iJ_{iyy}\,{}^i\omega_{iy} \\ -{}^iJ_{izz}\,{}^i\omega_{iz} & 0 & {}^iJ_{ixx}\,{}^i\omega_{ix} \\ {}^iJ_{iyy}\,{}^i\omega_{iy} & -{}^iJ_{ixx}\,{}^i\omega_{ix} & 0 \end{bmatrix} \begin{bmatrix} {}^i\omega_{ix} \\ {}^i\omega_{iy} \\ {}^i\omega_{iz} \end{bmatrix} \quad (13)$$
$$= X({}^iJ_i\,{}^i\omega_i)\,{}^i\omega_i$$

Similarly, the EJS for the forces called EJS-F is as equation:

$$M_{gyro-F} = {}^i\omega_i \times m_i\,{}^iv_{ci} \qquad (14)$$

where ${}^iv_{ci} = \begin{bmatrix} {}^iv_{cix} & {}^iv_{ciy} & {}^iv_{ciz} \end{bmatrix}^T$.

In multiband notation, it has been shown that the EJS may be represented by a nonlinear three-port gyrator.
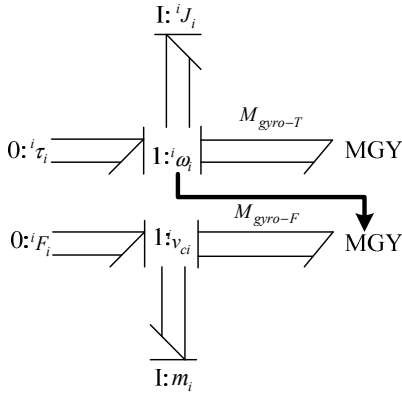
Fig. 14. Nonlinear 3-port gyrator composition of EJS

Fig. 15 shows the detailed bond graph representations according to the Newton-Euler's equations.

(a)

(b)
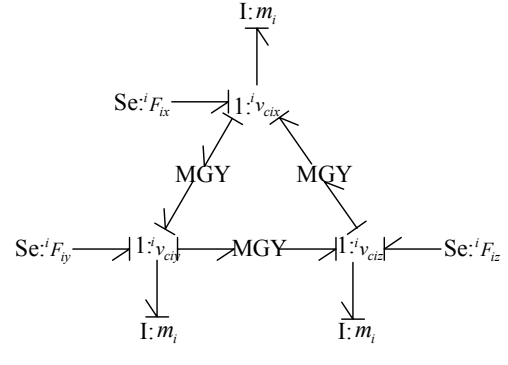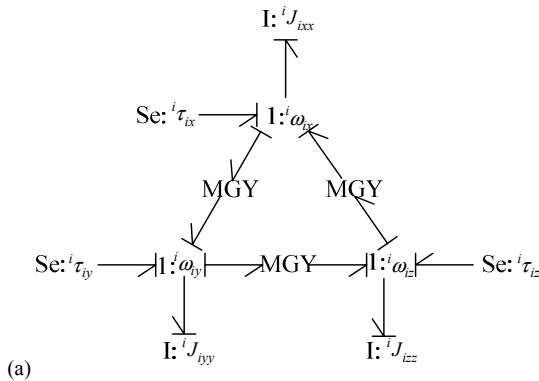
Fig. 15. Bond graph model of the Newton-Euler's equations (a) EJS-T (b) EJS-F

5) Bond Graph Modeling of a Link with a Joint

The bond graph model of a link including a joint module is illustrated in Fig. 16. This model is derived based on the exchange of power and movement between the constituents of the physical system corresponding to the Newton–Euler formulation. To represent the dynamics of a link with a joint, the bond graph of Fig. 16 is augmented with inertia elements, and the linear velocity of the centre of mass is described. First, an external velocity source Sf is supposed to act on the 0-junction as the motor angular velocity. At the left side the diagonal moment of inertia matrix ${}^iJ_i$ is connected as an I-element to the l-junction of the rotational velocities in the body frame. At the right side the mass matrix m_i is connected as an I-element to the l-junction of the translational velocities in the body-fixed frame, together with the gravity force source Se. The gyroscopic forces which act between these velocities are represented by the modulated gyrator MGY. Because the Euler equations represent these forces, the MGY is referred to as an EJS. The meanings of all the transformers MTF are shown in Fig. 16.
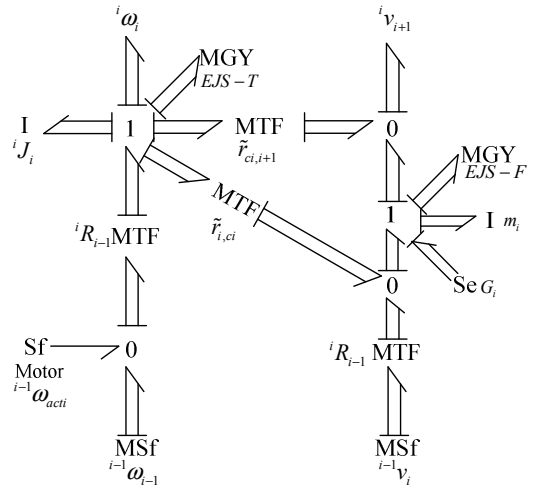
Fig. 16. Bond graph representing the dynamics of link *i*

D. Connection between the Mobile Platform and the Robotic Manipulator

Fig. 17 shows the bond graph model which connects the manipulators with the mobile platform. The blocks

Proceedings of the 1st International and 16th National Conference on Machines and Mechanisms (iNaCoMM2013), IIT Roorkee, India, Dec 18-20 2013

67

"wheel *i*" and "link 1" are the submodels containing the model of a conventional wheel and a link as discussed earlier. The mobile platform consists of two wheels and a base. All the forces applied by the wheels to the base can be summed. In the bond graph language, this is represented by a 1-junction. The *Sf* elements (Sf_l and Sf_r) are the flow sources which apply the angular velocities to the axis of the wheels. A *R* element (resistance) and a *C* element (stiffness) can be found in the model. These elements only act in the *z* direction of the base and represent the contact with the floor. Since the floor is very stiff and has a high resistance, the values of these two components are high. Without these elements, the robot model will accelerate in the negative *z* direction due to the gravity.
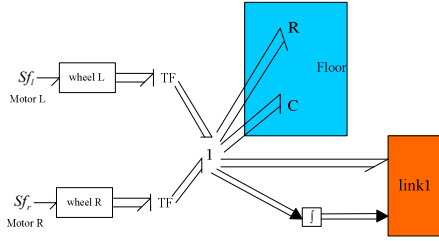
Fig. 17. Bond graph model of connection between mobile platform and manipulators

As described above, the mobile platform is connected to the first link of the robotic manipulator (the waist). However, in the bond graph model they cannot be connected directly. The model of the mobile platform provides rotation and translation to the first link. These velocities are applied in a point of the link. ^0R_B is the rotation matrix between the first link (frame $\sum_0$) and the world coordinate frame (frame $\sum_B$). $^B\omega_0$ and $^Bv_0$ are the angular velocity and the linear velocity of the connecting point between the platform and the first link and written in the world coordinate frame.

Angular velocity of joint 1 expressed in frame $\sum_1$:

$$^1\omega_1 = {}^1R_0({}^0\omega_0 + {}^0\omega_{act1}) = {}^1R_0\,{}^0R_B\,{}^B\omega_0 + {}^1R_0\,{}^0\omega_{act1} \quad (15)$$

Linear velocity of joint 1 expressed in frame $\sum_1$:

$$^1v_1 = {}^1R_0\,{}^0v_0 = {}^1R_0\,{}^0R_B\,{}^Bv_0 \quad (16)$$

Since the position of the base is required in calculating ^0R_B, an $\int$-block has to be added. This block calculates the position based on the current position and the rotation of the base.

V. VALIDATION OF BOND GRAPH MODEL

In this section, a toolbox BG V.2.1 in Matlab/Simulink is used for simulation and validation. Though many bond graph-based simulation software packages are available, at academic institutions level and in most industries, Matlab/Simulink is the software which is used more often for studying dynamical systems. Using this toolbox the bond graph model is directly built in Simulink. This toolbox only consists of 9 blocks which wholly realize the necessary functionality. Fig. 18 shows the bond graph model of one link using this toolbox. By comparison, it is obvious that this model is consistent with the bond graph model shown in Fig. 16.
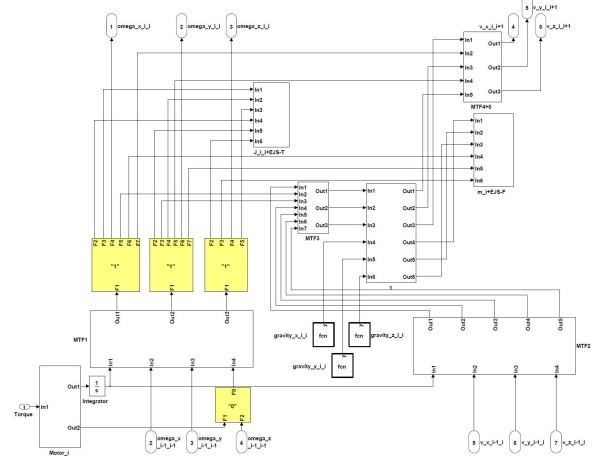
Fig. 18. Bond graph model of using BG V.2.1

In this section we will validate the bond graph model of the mobile manipulator excluding the hands. Neglecting the motions of the neck, this simplified robot has 18 DOFs (a 2 DOFs mobile platform, a 2 DOFs waist and two 7 DOFs arms). We know that, considering a typical wheeled mobile manipulator subject to kinematic constraints, the dynamics can be obtained in the form:

$$M(q)\ddot{q} + C(q,\dot{q})\dot{q} + F(q) + A^T(q)\lambda + \tau_d = E(q)\tau \quad (1)$$

where *r* kinematic constraints are described by:

$$A(q)\dot{q} = 0, \quad (2)$$

and $q \in \Re^p$ denotes the *p* generalized coordinates, $M(q) \in \Re^{p \times p}$ is a symmetric and positive definite inertia matrix, $C(q,\dot{q}) \in \Re^{p \times p}$ is a centripetal and Coriolis matrix, $F(q,\dot{q}) \in \Re^p$ is a friction and gravity vector, $A(q) \in \Re^{r \times p}$ represents a constraint matrix, $\lambda \in \Re^r$ is the Lagrange multiplier vector which denotes the constraint forces, $\tau_d \in \Re^p$ denotes unknown bounded disturbances including unstructured dynamics, $E(q) \in \Re^{p \times (p-r)}$ is the input transformation matrix, and $\tau \in \Re^{p-r}$ is a torque input vector.

Assume that all the parameters of the mobile manipulator are known and no disturbances. Based on the accurate mathematical dynamic model, an open-loop control system is established to obtain the joint torques. We apply these torques as the inputs of the bond graph model to track the reference trajectories. Let the desired output trajectories be specified as follows:

Proceedings of the 1st International and 16th National Conference on Machines and Mechanisms (iNaCoMM2013), IIT Roorkee, India, Dec 18-20 2013

68

The reference velocity vector for the mobile platform is designed as: $\begin{bmatrix} v_d & \omega_d \end{bmatrix}^T = \begin{bmatrix} 0.1t & 0.05t \end{bmatrix}^T$.

Meanwhile, the reference trajectories for the onboard waist and arms are given by:

$$q_{w1d} = 0.1t^2, q_{w2d} = 0.2t^2, q_{r1d} = 0.3t^2, q_{r2d} = 0.4t^2,$$
$$q_{r3d} = 0.5t^2, q_{r4d} = 0.6t^2, q_{r5d} = 0.7t^2, q_{r6d} = 0.8t^2,$$
$$q_{r7d} = 0.9t^2, q_{l1d} = -0.3t^2, q_{l2d} = -0.4t^2, q_{l3d} = -0.5t^2,$$
$$q_{l4d} = -0.6t^2, q_{l5d} = -0.7t^2, q_{l6d} = -0.8t^2, q_{l7d} = -0.9t^2$$

Numerical simulation results illustrated in Fig. 19 show that the desired trajectories are well tracked through the open-loop control system. This indicates that the bond graph model of the dual-arm mobile manipulator is identical with the mathematical model. The results also demonstrate the usefulness of the bond graph approach in modeling a complex system.
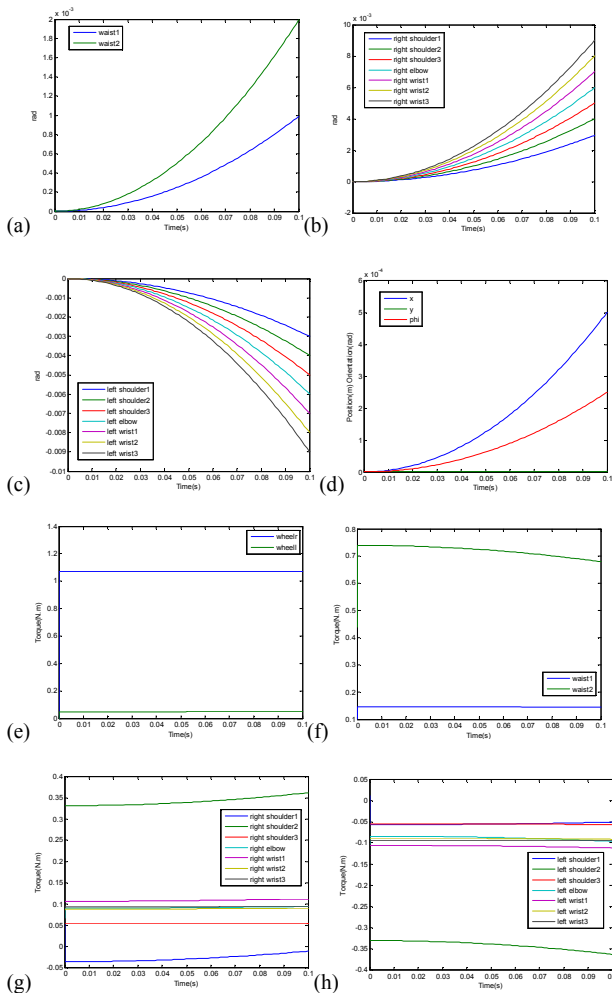
Fig. 19. Simulation results (a) Joint angles of waist (b) Joint angles of right arm (c) Joint angles of left arm (d) Posture of mobile platform (e) Joint torques of wheels (f) Joint torques of waist (g) Joint torques of right arm (h) Joint torques of left arm

VI. CONCLUSIONS

The objective of this paper is to introduce an approach for constructing a bond graph model of a dual-arm mobile manipulator. We have presented a step by step procedure for the bond graph modeling of this robot. The complete robot simulation structure is implemented in Simulink. The model has been validated under an open-loop controller through the precise mathematical model to show its effectiveness. It is proved that the application of bond graph method facilitates modeling of this complex electromechanical system, as well as extension of a control system.

REFERENCES

[1] Y. Yamamoto and X. Yun, "A modular approach to dynamic modeling of a class of mobile manipulators," International Journal of Robotics and Automation, vol. 12, no. 2, pp. 41-48, 1997.

[2] Q. Yu, I. M. Chen, "A general approach to the dynamics of nonholonomic mobile manipulator systems," ASME J. Dyn. Syst. Meas. Control 124, 512–521, 2002.

[3] H. G. Tanner and K. J. Kyriakopoulos, "Mobile manipulator modeling with Kane's approach," Robotica, vol. 19, pp. 675-690, 2001.

[4] L. Sheng, A. A. Goldenberg, "Neural-network control of mobile manipulators," IEEE Transactions on Neural Networks, vol. 12, no. 5, pp. 1121-1133, 2001.

[5] Y. Yamamoto and X. Yun, "Unified analysis on mobility and manipulability of mobile manipulators," in Proc. IEEE International Conference on Robotics and Automation, pp. 1200–1206, 1999.

[6] Y. Yamamoto, X. Yun, "Coordinating locomotion and manipulation of a mobile manipulator," in Proc. the 31th Conference on Decision and Control, Tucson, AZ, pp. 2643-2648, Dec.1992.

[7] J. Chung, S. Velinsky, "Robust control of a mobile manipulator-dynamic modelling approach," Proceedings of the American Control Conference, pp. 2435-2439, San Diego, California, USA, 1999.

[8] Q. Yu, I. Chen, "A general approach to the dynamics of nonholonomic mobile manipulator systems," ASME Trans. of Dynamic Systems, Measurement, and Control, Vol. 124, No. 4, pp. 512-521, 2002.

[9] H. Tanner, K. Kyriakopoulos, "Mobile manipulator modelling with Kane's approach," Robotica, Vol. 19, pp. 675-690, 2001.

[10] W. Jingguo, L. Yangmin, "Dynamic modeling of a mobile humanoid robot," In IEEE Int. Conf. on Robotics and Biomimetics, Bangkok, Thailand, pp. 639-644, 2009.

[11] P. C. Breedveld, "Port-based modeling of mechatronic systems," Mathematics and Computers in Simulation, Selected papers from the 4th IMACS Symposium on Mathematical Modelling, 66 (2-3), pp. 99-128, 2004.

[12] Wolfgang Borutzky, Bond Graph Methodology, Springer, 2010.

[13] A. Mukherjee, R. Karmakar, Modeling and Simulation of Engineering Systems through Bondgraphs, Narosa Publishing House, New Delhi, 2000.

[14] Mutku Mvengei and john Kihiu, "Bond graph modeling of mechanical dynamics of an excavator for hydraulic system analysis and design," International Journal of Aerospace and Mechanical Engineering, 3:4, 2009.

[15] Dresscher, Douwe and Brodskiy, Yury and Breedveld, Peter and Broenink, Jan and Stramigioli, Stefano, "Modeling of the youBot in a serial link structure using twists and wrenches in a bond graph," In 2nd International Conference on Simulantion, Modeling, and Programming for Autonomous Robots, SIMPAR 2010 Workshops, 15-18 November 2010, Darmstadt, Germany.

[16] Y. Yamamoto, X. Yun, Coordinating locomotion and manipulation of a mobile manipulator, in Proc. the 31th Conference on Decision and Control, Tucson, AZ, pp. 2643-2648, Dec.1992.

[17] J. J. Craig, Introduction to Robotics, Addison Wesley, second ed., 1989.

Proceedings of the 1st International and 16th National Conference on Machines and Mechanisms (iNaCoMM2013), IIT Roorkee, India, Dec 18-20 2013

69